MIT Open Access Articles

Flowing plasmas and absorbing objects: analytic and numerical solutions culminating 80 years of ion-collection theory

Massachusetts Institute of Technology

Flowing plasmas and absorbing objects: analytic and numerical solutions culminating 80 years of ion-collection theory

Flowing plasmas and absorbing objects: analytic and numerical solutions culminating 80 years of ion-collection theory

I H Hutchinson and L Patacchini

Plasma Science and Fusion Center, Massachusetts Institute of Technology, Cambridge, MA, USA

E-mail: ihutch@mit.edu

Abstract
Recent computational and theoretical progress in understanding and calculating ion collection by negatively charged absorbing objects in a flowing plasma is outlined. The results are placed in the context of key theoretical achievements of prior research. Despite the topic's long history, and past profound insights, fully rigorous quantitative solution of the non-linear, multidimensional, self-consistent, kinetic-theory problem has not until recently been feasible. Now we are able to establish the adequacy or inadequacy of approximate treatments, and provide critical quantitative results. In the process, some qualitative surprises have also emerged.

(Some figures in this article are in colour only in the electronic version)

Since Tonks and Langmuir [1] first addressed the acceleration of ions during collection by Langmuir probes, the interaction of even the simplest spherical absorbing objects with plasmas has been a major challenge to theory. The physics is common to a variety of applications, such as the interaction of space-craft or planetary bodies with the surrounding plasma, the behavior of dust in gas discharges and the understanding of probes, especially Mach probes, in magnetic-confinement plasmas. The inherent non-linearity and non-Maxwellian ion velocity distribution were addressed by numerical kinetic solutions for the 1D spherically symmetric collisionless case in the 1960s. Yet symmetry-breaking plasma flow and collisions were mostly addressed only using heuristic approximations until multidimensional, Monte Carlo, computational solutions became feasible.

The Specialized Coordinate, Particles and Thermals in Cell ('SCEPTIC') code [2, 3] was written specifically to enable accurate PIC solutions to be obtained for a spherical object in a flowing plasma. It solves self-consistently the evolution (typically to statistical steady state) of the six-dimensional phase-space distribution of perhaps 7 million ions moving in an electric potential (ϕ) that satisfies the Poisson equation on a spherical grid in the presence of electron density given by a Boltzmann factor $n_e = n_\infty \exp(e\phi/T_e)$, where T_e is the constant
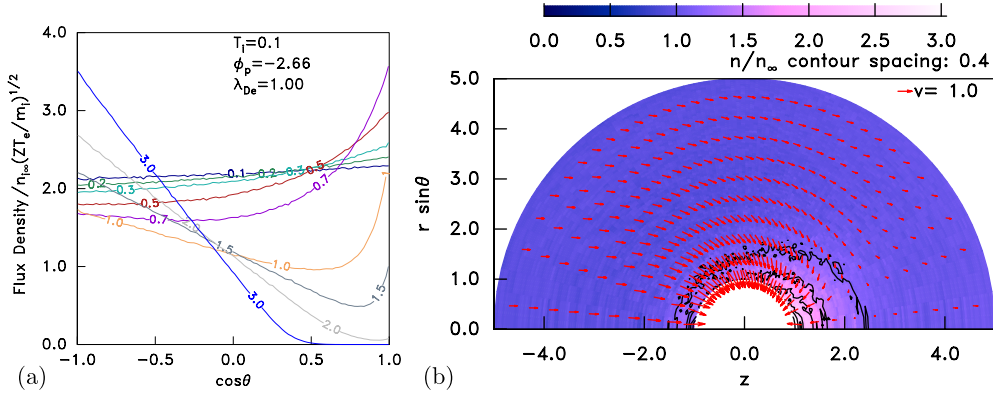
Figure 1. (*a*) Flux as a function of angle on the sphere (here floating) for different drift velocities (v_f line labels) shows strong reversal of asymmetry in some conditions: higher flux on the downstream side ($\cos\theta > 0$). This is caused by ion focusing behind the sphere raising the density there, as shown by the contours of density in the example (*b*) (for $v_f = 0.5$).

electron temperature. Ions leaving the computational domain at the inner or outer boundary are reinjected with statistics that represent the distribution function at infinity (usually a drifting Maxwellian), and outer boundary conditions are designed to provide accurate solutions with modest domain-size.

SCEPTIC was benchmarked against the analytic and prior numerical results for spherically symmetric (stationary plasma) cases and confirmed the finite Debye-length (λ_{De}) results of Laframboise [4] to an accuracy of a few tenths of a percent. Symmetric infinitesimal-λ_{De} (quasi-neutral) calculations [2] confirmed the potential distributions of classic works [5, 6], but revealed few-per cent-level inconsistencies in their flux values that have yet to be resolved.

The distribution of flux to the sphere surface, which is what is required to calibrate Mach-probes that try to measure plasma flow by observing with electrodes facing in different directions, was found to be describable by a simple formula in the quasi-neutral case that gives ion flux (Γ) ratio upstream to downstream, as

$$\Gamma_u / \Gamma_d = \exp(K v_f), \tag{1}$$

where v_f is the drift velocity normalized to $\sqrt{T_e/m_i}$ and K is a calibration factor that can be taken universally as $K = 1.34$ for $T_i/T_e \lesssim 3$. This result, which notably contradicts prior assumed ion-temperature dependence based on dubious heuristic arguments, has subsequently been experimentally verified [7]. The simple result proves not to apply to cases with finite Debye length [3] (compared with sphere size, λ_{De}/r_p). At small ion temperature, $T_i/T_e = 0.1$, even rather modest values, $\lambda_{De}/r_p \sim 0.02$, give substantial changes in the effective calibration, K; and for $0.1 < \lambda_{De}/r_p < 10$ the value of K is negative! This counter-intuitive enhancement of ion collection on the *downstream* side, illustrated in figure 1, means that unmagnetized spherical Mach-probes are problematic in this parameter regime.

SCEPTIC can readily calculate the ion drag force transmitted to the object [8]. It consists of three contributions to momentum flux across any bounding surface: the direct ion momentum flux, the Maxwell stress and the electron pressure. In steady state the total momentum flux (summing the contributions) is independent of radius, which serves as a useful code cross-check of momentum conservation. In the limit of large Debye length ($\lambda_{De}/r_p \gg 1$) the drag force calculation is equivalent to the standard electron–ion drag problem [9, 10], which gives rise to a Coulomb logarithm. The drag on a charged sphere is naturally expressed
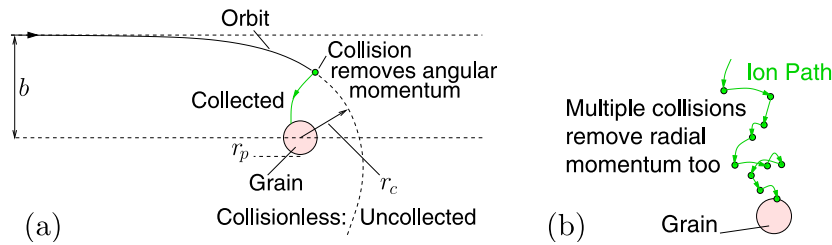
Figure 2. Collisions enhance collection by removing angular momentum (*a*), but eventually decrease it by removing radial momentum (*b*).

in the same form, except with a different Coulomb logarithm that takes account not only of the 90° scattering impact parameter, b_{90} and the screening length λ_s, but also the finite size of the sphere which determines a collection impact parameter b_c. The replacement [11] $\ln \Lambda \to \frac{1}{2} \ln[(b_{90}^2 + \lambda_s^2)/(b_{90}^2 + b_c^2)]$ becomes increasingly unsatisfactory for lower λ_{De}/r_p and a different heuristic approximation has been proposed [12]: $\ln \Lambda \to \ln[(b_{90} + \lambda_s)/(b_{90} + r_p)]$, which better fits collision cross-section calculations for Debye–Hückel potentials. SCEPTIC calculations [13] show that while the resulting formula works well when $T_i \sim T_e$, it is as much as a factor of 2 too low in the transonic flow regime ($0.4 \lesssim v_f \lesssim 2$) when $T_i/T_e \sim 0.01$, even for $\lambda_{De}/r_p \sim 20$. The discrepancy arises from complicated ion orbit effects that could hardly have been anticipated. A modified comprehensive analytic expression, fitted to SCEPTIC results, provides convenient drag force values across the full parameter ranges of collisionless plasmas [13].

Collisional effects are of importance in the conditions of typical dusty plasma experiments, because the neutral density is high. The effects of ion–neutral collisions on ion collection even with mean-free-path large compared with the object have long been argued to enhance collection. The basic mechanism is illustrated in figure 2(*a*), upon which heuristic estimates of the enhancement have been based [14]. The loss of angular momentum by collisions has also been invoked as a rationale for the limiting ABR [15] radial-motion approximation, in which angular motion is ignored. At long Debye length, ABR predicts an ion collection substantially greater than the orbital motion limited (OML) formula [16], which applies for collisionless orbits in these symmetric potentials. The difficulty with this rationale is that collisions also have a countervailing effect illustrated in figure 2(*b*) whereby the loss of *radial* momentum *decreases* the ion collection; so rigorous theory is essential. In the limit of large collisionality, continuum diffusion/mobility treatment of the ions gives a convincing rigorous approach [18], which shows the anticipated flux-decrease. Recent rigorous kinetic-theory calculations [17] in the low-collisionality (flux-enhancing) regime are accurate to first order in the collision frequency (ν_c). In between, a numerical approach like SCEPTIC seems unavoidable. Actually for this spherically symmetric case SCEPTIC's multidimensional capability is not required, but the calculations are a good test of the accuracy of its collisional treatment. As figure 3 shows, the agreement of SCEPTIC with the rigorous calculations is excellent in their regimes of validity [19]. Moreover, SCEPTIC shows that the ABR value is approximately equaled at the peak of the curve of flux versus collisionality—but only there.

The collisional effects on ion drag have provoked substantial interest recently because the drag has been observed to reverse sign in some simulations [20], and can be shown analytically to reverse in the high-collisionality limit [21, 22]. SCEPTIC quantitatively confirms the reversal of drag at high ν_c, as figure 4 illustrates. However, in that regime the reversal is not of
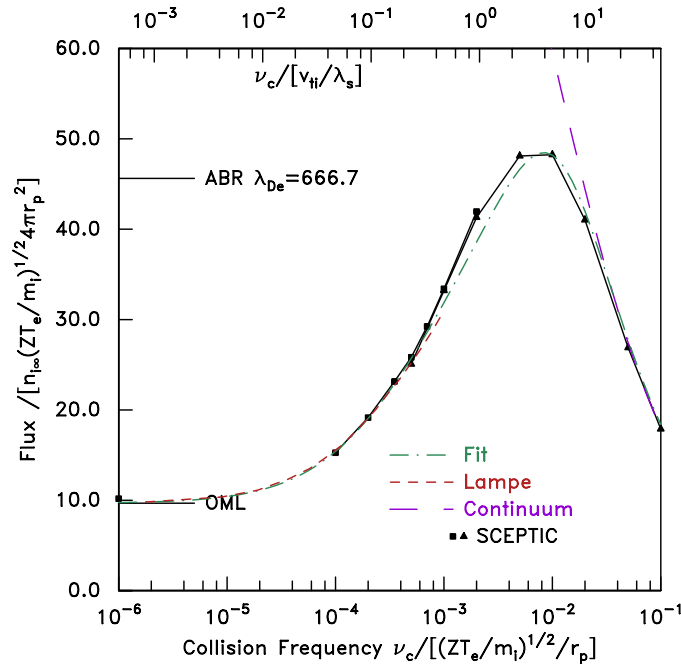
Figure 3. Flux collection as a function of collisionality with $T_i/T_e = 0.01$ for a floating sphere in Ar$^+$. Points are SCEPTIC values, compared with the OML and ABR values, the Lampe *et al*, low collisionality approximation [17] and with the continuum high-collisionality approximation [18]. A convenient universal analytic fit to SCEPTIC is also plotted. See [19].

much interest because the drag force is overwhelmed by other much greater forces. SCEPTIC contradicts the claims of drag reversal at modest collisionality. It does not occur [23].

Magnetic field can be incorporated into the two-dimensional SCEPTIC calculations if it is in the same direction as the external drift, so that axisymmetry remains. Calculations at moderate degrees of magnetization [24] have been compared with some of the classic bounds derived analytically [25–27]. The results are broadly consistent, but of course SCEPTIC gives actual values not just bounds. We find the reduction in flux to be proportional to the field strength at low field, not B^2, as has erroneously been stated [26]. A major problem with axisymmetric magnetized calculations is that perfect conservation of axial canonical angular momentum prevents any cross-field transport, with the result that the presheath rapidly extends along the field, as field strengthens, reaching to the computational boundary. This is a real physics issue, not just a computational problem. Magnetized ion collection depends upon the cross-field ion transport, however small [28], and so the collisionless axisymmetric model is really an inadequate representation. Consequently one must really proceed to a fully 3D situation, where the external ion drift, in addition to any parallel component, has a component perpendicular to the magnetic field, which breaks the axisymmetry. We have therefore built a new version of the code which calculates on the basis of a fully 3D potential: SCEPTIC3D. It naturally requires substantially greater computational resources, running with typically 50 million particles. We illustrate an example of the computed flux variation around the probe surface in figure 5, when the plasma is quasi-neutral.

A related new discovery is that one can obtain analytic solutions of the interaction of a perpendicularly convecting, strongly magnetized plasma (in which the Larmor radius is much
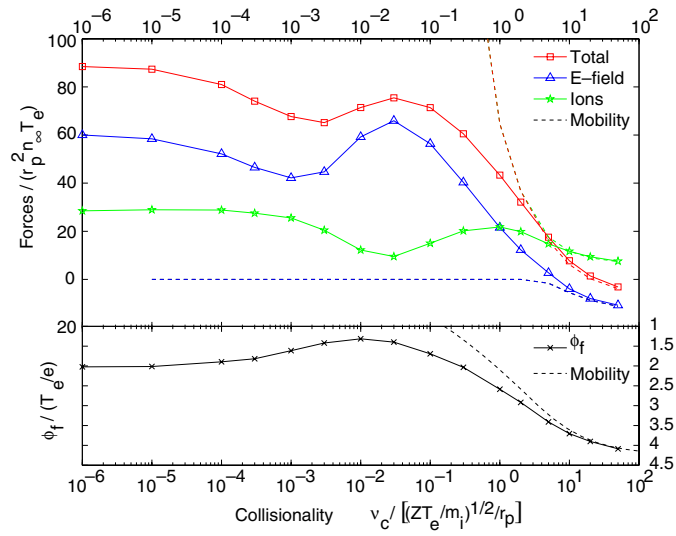
Figure 4. Example of the variation of the ion drag force and floating potential as a function of collisionality for a floating sphere, in hydrogen plasma with $T_i/T_e = 0.01$, $v_f = 1$ and $\lambda_{De} = 20r_p$. Only for the highest collisionality, into the continuum regime where the mobility approximation is reached, does the total drag force reverse. From [23].
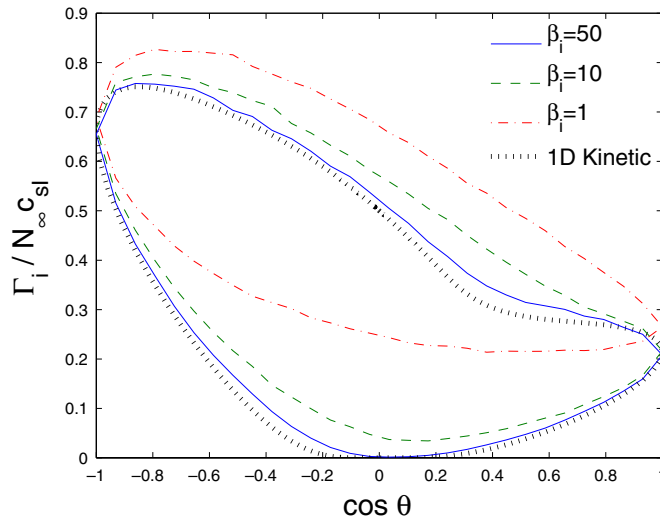

Figure 5. The variation of flux density to the sphere with angle around a great circle in the plane of field and drift velocity, for several values of normalized magnetic field $\beta = r_p/\rho_i$. $T_i/T_e = 1$, $v_{f\parallel} = v_{f\perp} = 1/\sqrt{2}$. From [29].

smaller than the object size: $\rho_i \ll r_p$) with an object of arbitrary shape [30]. This approximation of uniform external perpendicular velocity contrasts with prior treatments that invoke a heuristic transverse anomalous diffusion. It affords a rigorous solution based on fundamental physics. The solution is exceptionally compact under the assumption of isothermal ions, which can be treated via fluid drift-approximation, leading to hyperbolic equations amenable to the 'method
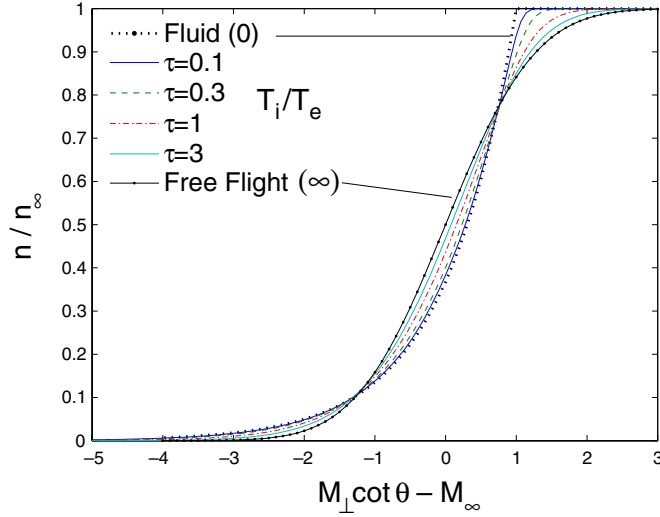
Figure 6. Vlasov solution for the density as a function of characteristic angle, θ, for different external temperature ratios. The analytic limits are also illustrated. From [32].

of characteristics'. One of the characteristics proves to be a straight line through the point in question, tangential to the surface of the object in the plane of perpendicular drift and magnetic field. Along this line, the parallel Mach number $M_\parallel$ and the ion density n are constant, and have values determined by the characteristic's angle θ to the direction of the field, in the form

$$M_\parallel = M_\perp \cot\theta - 1, \qquad \ln n = \ln n_\infty - M_\parallel + M_{\parallel\infty}, \qquad (2)$$

where $M_\perp$ is the (external) perpendicular Mach number $v_\perp/c_s$ and $M_{\parallel\infty}$ is the external parallel Mach number of background flow. The ion flux to the object, per unit area perpendicular to the field, is then

$$\Gamma_\parallel = n c_s = n_\infty c_s \exp(-1 - M_\parallel + M_\perp \cot\theta). \qquad (3)$$

A critical part of this rigorous solution is that it is valid *taking into account the drifts arising from the plasma perturbation by the object* [31], even though those drifts do not appear in the final expressions. The physical reason for this remarkable result is that the drifts are always perpendicular to ∇n. This means that the additional drifts are always along contours of constant n, and since the $M_\parallel$ is a function of n, those contours are also contours of constant $M_\parallel$. Consequently, zero additional convective derivative arises from the additional drifts. They can be ignored in obtaining the spatial dependence. For essentially the same underlying reasons, a semi-analytic solution of the full (parallel-direction) Vlasov kinetic equation can be obtained, as a function of space [32]. It gives fluxes that would be indistinguishable from the fluid result (equation (3)) in most experimental situations, but as T_i/T_e becomes larger, it eventually tends to the 'free-flight' limit where ion acceleration can be ignored. Figure 6 shows the solution, as a function of the angle (θ) of the tangential characteristic (which at the surface is the surface-angle) to the magnetic field.

The analytic results are compared [29] with the solution obtained from SCEPTIC3D for the equivalent parameters in figure 7. For all of space below $y = 1$, the rearmost point of the object, the contours of density show excellent agreement. The small discrepancies on the leading edge of the object arise because the ion Larmor radius is finite (though small) in the PIC simulations, while the analytic treatments take $\rho_i = 0$. The analytic treatments are valid
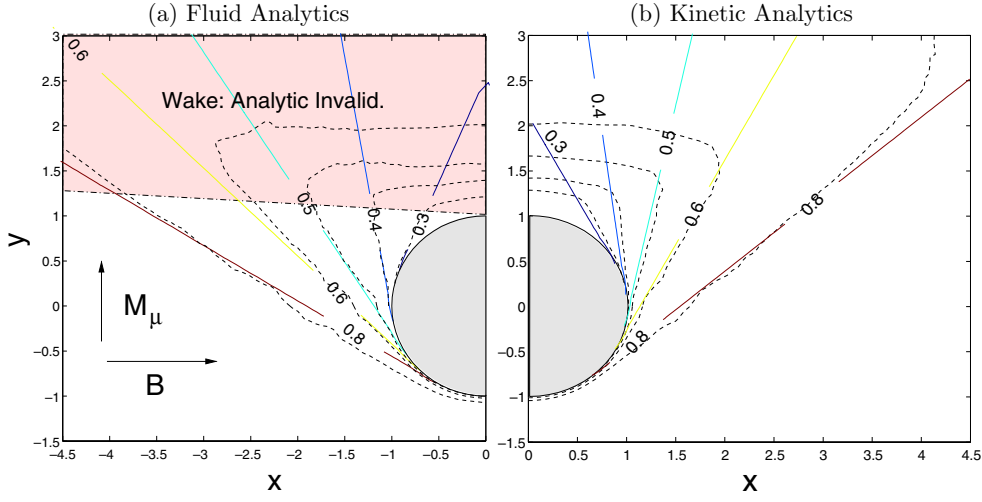
Figure 7. Comparison of density (n/n_∞) contours for analytic ($r_p/\rho_i = \infty$) (solid) and SCEPTIC ($r_p/\rho_i = 20$) (dashed) solutions. Parameters are $M_\parallel = 0$, $\lambda_{De} = 0$; (a) $T_i/T_e = 0.1$, $M_\perp = 0.5$, fluid analytic values; (b) $T_i/T_e = 1$, $M_\perp = 1$, kinetic analytic values. After [29].

only in regions where ions do not arrive simultaneously having passed either to the left or right of the object. Where the streams of ions merge, behind the object (at larger y) is, in the fluid sense, a shocked, wake region. SCEPTIC can fully treat that region, and shows the density contours closing behind the object.

The analytic fluid treatment extends also to situations in which the external diamagnetic drifts, arising from ∇n_∞, ∇T_e or ∇T_i, are significant [31]. These perpendicular drifts require retention of terms in the equations one order smaller in ρ_i/r_p than those of the $E \times B$ drifts so far discussed, and give rise to effects that require quantitative evaluation in order to discount. In addition there arise important contributions from displacements in the magnetic presheath (MPS) which must be retained. A relatively compact generalization of equation (3) that accounts for these effects results, giving the flux to the object per unit perpendicular area in normalized units:

$$\ln\left\{\frac{\Gamma_{\parallel p}}{n_\infty c_s}\right\} = \underbrace{-1 - M_{\parallel\infty}}_{\text{parallel flow}} + \left[\overbrace{\underbrace{M_E}_{E \times B} + M_{Di} + \underbrace{(1 + M_{\parallel\infty})M_{T_e}}_{T_e\text{-gradient effect}} - \underbrace{\left(\frac{1 - \sin\alpha}{1 + \sin\alpha}\right)M_D}_{\text{MPS effect}}}^{\text{perpendicular flow}}\right]\cot\theta \qquad (4)$$

In this formula, $\hat{\boldsymbol{y}}$-direction drifts are as follows. $M_E = [\boldsymbol{E} \times \boldsymbol{B}/c_s B^2] \cdot \hat{\boldsymbol{y}}$, the electric field drift, is in accord with intuition, and the previous form. $M_{Di} = [-\nabla p \times \boldsymbol{B}/(c_s n e B^2)] \cdot \hat{\boldsymbol{y}}$ is the total ion diamagnetic drift. $M_{T_e} = [\nabla T_e \times \boldsymbol{B}/(c_s e B^2)] \cdot \hat{\boldsymbol{y}}$ is the electron diamagnetic drift due to T_e gradient. $M_D = M_{Di} - M_{De}$ is the difference between ion and electron diamagnetic drifts. α is the angle between $\boldsymbol{B}$ and object surface. θ is the angle in the x–y-plane between $\boldsymbol{B}$ and the object surface. A Mach-probe, by measuring how the ion flux varies as a function of angle, θ, deduces the parallel flow and the perpendicular flow. The perpendicular flow that it deduces is the entire expression in the square brackets, which (in contrast to some past opinion) does include contributions from diamagnetic terms. These contributions have not yet been verified by experiment or simulation.

This convective treatment is more appropriate than the prior diffusive treatment for magnetized probes in the typical case where the size of eddies responsible for cross-field transport exceeds the size of the probe. Fortunately, the approximate Mach-probe calibration given by the diffusion approximation [28] is quantitatively almost the same as obtained rigorously in this convective treatment.

In summary, we now have the computational capability to solve the full non-linear, asymmetric, ion-collection problem, including the effects of collisions, external drifts and magnetic field. Analytic theory is not thereby made irrelevant. Critical comparisons enable both the validation of codes and the clarification of analytic strengths, weaknesses and approximations.

References

[1] Tonks L and Langmuir I 1929 *Phys. Rev.* **34** 876
[2] Hutchinson I H 2002 *Plasma Phys. Control. Fusion* **44** 1953
[3] Hutchinson I H 2003 *Plasma Phys. Control. Fusion* **45** 1477
[4] Laframboise J G 1966 Theory of spherical and cylindrical langmuir probes in a collisionless Maxwellian plasma at rest *Technical Report* 100, (*Doctoral Dissertation*) University of Toronto Institute for Aerospace Studies
[5] Al'pert Ya L, Gurevich A V and Pitaevskii L P 1965 *Space Physics with Artificial Satellites* (New York: Consultants Bureau)
[6] Parrot M J M, Storey L R O, Parker L W and Laframboise J G 1982 *Phys. Fluids* **25** 2388
[7] Ando A, Watanabe T K, Makita T, Tobari H, Hattori K and Inutake M 2006 *Contrib. Plasma Phys.* **46** 335–40
[8] Hutchinson I H 2005 *Plasma Phys. Control. Fusion* **47** 71
[9] Chandrasekhar S 1943 *Astrophys. J.* **97** 255
[10] Spitzer L 1962 *Phyics of Fully Ionized Gases* (New York: Interscience) 2nd edn
[11] Shukla P K and Mamun A A 2002 *Introduction to Dusty Plasma Physics* (Bristol: Institute of Physcis Publishing)
[12] Khrapak S A, Ivlev A V, Zhdanov S K and Morfill G E 2005 *Phys. Plasmas* **12** 042308
[13] Hutchinson I H 2006 *Plasma Phys. Control. Fusion* **48** 185
[14] Zakrzewski Z and Kopiczinski T 1974 *Plasma Phys.* **16** 1195
[15] Allen J E, Boyd R L F and Reynolds P 1957 *Proc. Phys. Soc.* B **70** 297
[16] Mott-Smith H M and Langmuir I 1926 *Phys. Rev.* **28** 727
[17] Lampe M, Goswami R, Sternovsky Z, Robertson S, Gavrishchaka V, Ganguli G and Joyce G 2003 *Phys. Plasmas* **10** 1500
[18] Chang J-S and Laframboise J G 1976 *Phys. Fluids* **19** 25
[19] Hutchinson I H and Patacchini L 2007 *Phys. Plasmas* **14** 13505
[20] Schweigert I V, Alexandrov A L and Peeters F M 2004 *IEEE Trans. Plasma Sci.* **32** 623–6
[21] Khrapak S A, Klumov B A and Morfill G E 2007 *Phys. Plasmas* **14** 034502
[22] Hutchinson I H 2007 *Phys. Plasma* **14** 074701
[23] Patacchini L and Hutchinson I H 2008 *Phys. Rev. Lett.* **101** 025001
[24] Patacchini L and Hutchinson I H 2007 *Plasma Phys. Control. Fusion* **49** 1719–33
[25] Parker L W and Murphy B L 1967 *J. Geophys. Res.* **72** 1631
[26] Rubinstein J and Laframboise J G 1982 *Phys. Fluids* **25** 1174–82
[27] Sonmor L J and Laframboise J G 1991 *Phys. Fluids* B **3** 2472–90
[28] Hutchinson I H 2002 *Principles of Plasma Diagnostics* (Cambridge: Cambridge University Press) 2nd edn
[29] Patacchini L and Hutchinson I H 2010 *Plasma Phys. Control. Fusion* **52** 035005
[30] Hutchinson I H 2008 *Phys. Rev. Lett.* **101** 035004
[31] Hutchinson I H 2008 *Phys. Plasmas* **15** 123503
[32] Patacchini L and Hutchinson I H 2009 *Phys. Rev.* E **80** 036403